Carnegie Observatories Astrophysics Series, Vol. 3:
Clusters of Galaxies: Probes of Cosmological Structure and Galaxy Evolution, 2004
ed. J. S. Mulchaey, A. Dressler, and A. Oemler (Pasadena; Carnegie Observatories:
http://www.ociw.edu/ociw/symposia/series/symposium3/proceedings.html)

Comparing Local and High-z X-ray Galaxy Clusters: Properties of the Gas Mass Fraction, Metallicity, and Entropy

S. ETTORI[1], P. TOZZI[2], and P. ROSATI[1]
(1) European Southern Observatory, Garching b. Munchen (Germany)
(2) INAF, Trieste, Italy

Abstract

We summarize here some of the results on the properties of the X-ray emitting plasma in galaxy clusters at high redshift that we present and discuss in a series of papers (Ettori, Tozzi & Rosati 2003a; Tozzi et al. 2003; Rosati et al. 2003; Ettori et al. 2003b). In particular, we report on (1) how the gas mass fraction measured in galaxy clusters at $z > 0.7$ is used to put significant constraints on the cosmological parameters in a independent and complementary way with respect to the power spectrum of the observed anisotropies in the Cosmic Microwave Background and the magnitude-redshift relation for distant type Ia supernovae (Ettori et al. 2003a), (2) what is the measured metallicity of the intracluster medium at redshift between 0.3 and 1.3 (Tozzi et al. 2003, Rosati et al. 2003), (3) how the observed entropy values in the cores of these high$-z$ systems compare with local estimates (Ettori et al. 2003b).

1.1 How We Constrain the Cosmological Parameters Using $f_{\rm gas}$

Several tests have been suggested to constrain the geometry and the relative amounts of the matter and energy constituents of the Universe (e.g. Peebles & Ratra 2002). A method that is robust and complementary to the others makes use of the gas mass fraction, $f_{\rm gas} = M_{\rm gas}/M_{\rm tot}$, as inferred from X-ray observations of clusters of galaxies through the measurements of the surface brightness profile and an emission-weighted gas temperature. For each galaxy cluster in our sample observed at redshift z, we evaluate the gas mass fraction at r_Δ, $f_{\rm gas}(r_\Delta) = M_{\rm gas}(< r_\Delta)/M_{\rm tot}(< r_\Delta)$, where r_Δ is defined according to the dark matter profile, $M_{\rm tot}(< r)$, for a fixed density contrast $\Delta = M_{\rm tot}(< r_\Delta)/(4\pi \rho_{\rm c,z} r_\Delta^3)$, where $\rho_{\rm c,z}$ is the critical density at redshift z.

For a grid of values of $(\Omega_{\rm m}, \Omega_\Lambda, w)$ (w is the ratio between the pressure and the energy density in the equation of state of the dark energy component, e.g. Wang & Steinhardt 1998), we evaluate $f_{\rm gas}(r_\Delta)$ considering its dependence upon the cosmological parameters and redshift, that is present in (i) $f_{\rm gas} \propto$ *(angular diameter distance)*$^{3/2}$ and (ii) the density contrast, Δ.

We constrain the cosmological parameters making the two assumptions that (1) the relative amount of baryons with respect to the total mass observed in galaxy clusters is rep-

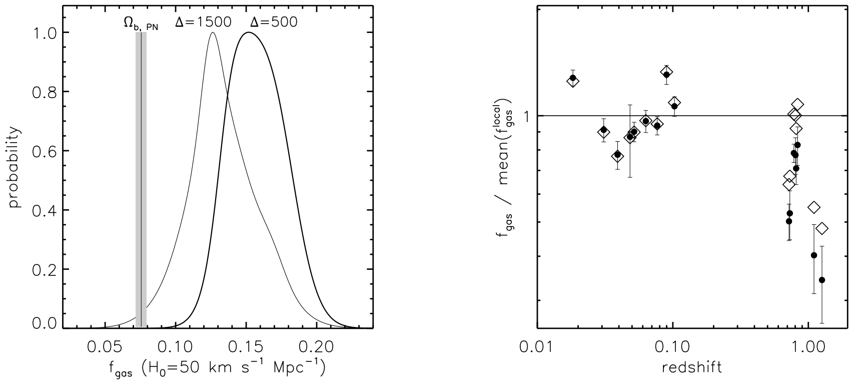

Fig. 1.1. Cosmological constraints by using $f_{\rm gas}$: *(left panel: 1st method:* $\Omega_{\rm m}$ *from baryon fraction)* Probability distributions (see Press 1996) at different density contrast Δ of the values of the $f_{\rm gas}$ for relaxed nearby clusters with $T_{\rm gas} > 4$ keV. The central and $1-\sigma$ values are $(0.126, 0.024)$ and $(0.152, 0.020)$ at Δ = 1500 and 500, respectively. The estimated $\Omega_{\rm b}$ from primordial nucleosynthesis results (Burles et al. 2001) is overplotted for comparison. *(Right panel: 2nd method:* $f_{\rm gas}$ *constant in time)* Distribution as function of redshift of the gas fraction relative to the mean local value and estimated for the clusters in our sample at the same overdensity Δ =1500. *Filled circles* are the values calculated in an Einstein-de Sitter universe, whereas *diamonds* indicate the results for a low density universe ($\Omega_{\rm m} = 1-\Omega_\Lambda = 0.3$).

resentative of the cosmic baryon fraction (e.g. White et al. 1993), (2) the gas fraction is constant in time (e.g. Sasaki 1996). In particular, we use deprojected X-ray spectral results of *BeppoSAX* observations of a sample of nearby galaxy clusters (Ettori, De Grandi & Molendi 2002) to set constraints on the dynamical estimate of $\Omega_{\rm m}$ using the cluster baryon fraction. We then analyze *Chandra* observations of a sample of eight distant clusters with redshift in the range 0.72 and 1.27 and evaluate the geometrical limits on the cosmological parameters $\Omega_{\rm m}$, Ω_Λ and w by requiring that the gas fraction remains constant with redshift (see Figure 1.1).

1.1.1 Results on the Best-fit Values of $(\Omega_{\rm m}, \Omega_\Lambda, w)$

We present our cosmological constraints in Figure 1.2. By combining the two independent probability distributions given from the two methods described above, and using *a priori* distributions on both $\Omega_{\rm b}$ and H_0 peaked around primordial nucleosynthesis (Burles et al. 2001) and HST-Key Project results respectively (Freedman et al. 2001), we obtain that, at 95.4 per cent level of confidence, (i) $w < -0.49$, (ii) $\Omega_{\rm m} = 0.34^{+0.11}_{-0.05}$, $\Omega_\Lambda = 1.30^{+0.44}_{-1.09}$ for $w = -1$ (corresponding to the case for a cosmological constant), and (iii) $\Omega_{\rm m} = 1-\Omega_\Lambda = 0.33^{+0.07}_{-0.05}$ for a flat Universe. By combining these results with the magnitude-redshift relation for distant type Ia supernovae (Garnavich et al. 1998, Leibundgut 2001), we further constrain $\Omega_\Lambda = 0.94^{+0.28}_{-0.32}$ and $w < -0.89$ at the 2σ level (thick solid contours in Fig. 1.2).

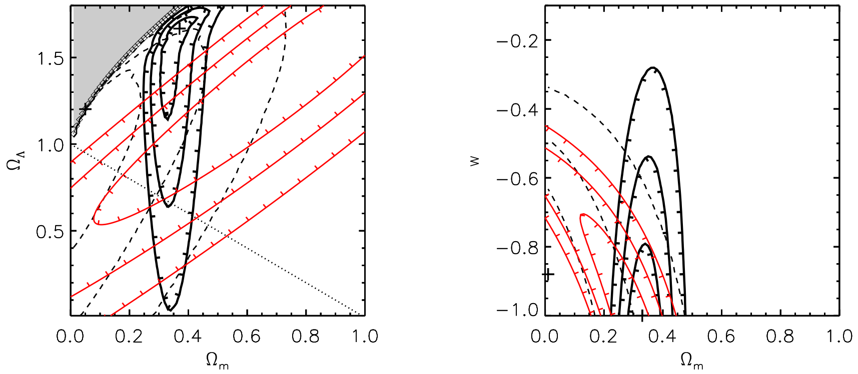

Fig. 1.2. Constraints on the cosmological parameters (1, 2 and 3 σ confidence contours). Dashed lines: by using only $f_{\rm gas}$; light solid lines: from the magnitude-redshift relation of SN Ia; dark/thick solid lines: by combining $f_{\rm gas}$ and SN Ia methods.

1.2 Metallicity in the ICM at High Redshift

We analyze 18 hot ($3 < kT < 8$ keV) galaxy clusters with redshift $0.3 < z < 1.3$, most of them observed with *Chandra* . For two of the $z > 1$ clusters, we also use deep *XMM-Newton* observations. Our analysis aims at deriving the Iron abundance of the ICM at the highest redshift probed to date. We find that $Z_{\rm Fe} = 0.25 \pm 0.05 Z_{\odot}$ at $< z > \approx 0.8$, consistent with the local canonical metallicity value of about $0.3 Z_{\odot}$ (see Figure 1.3). Medium and low temperature clusters ($kT < 5$ keV) tend to have larger Iron abundances than hot clusters. At redshift of about 1.2 (four clusters at $z > 1$ are in our sample), we obtain a statistically significant detection of the Fe-K line in only one object ($Z_{\rm Fe} > 0.10 Z_{\odot}$ at the 90 per cent c.l.). Combining all the current dataset from *Chandra* ad *XMM-Newton* at $z > 1$, the average metallicity is measured to be $Z_{\rm Fe} = 0.21^{+0.10}_{-0.05} Z_{\odot}$ (1σ), thus suggesting that no evolution of the mean Iron abundance is present out to $z \approx 1.2$.

1.3 Entropy Values in the Cores of High−z Galaxy Clusters

We present in Ettori et al. (2003b) a study of the integrated physical properties of a sample of 26 X-ray galaxy clusters observed with *Chandra* at redshift between 0.4 and 1.3, with particular emphasis on the properties and evolution of the X-ray scaling laws. As part of that project, we have also determined the values of the quantity $S = T_{\rm gas}/n_{\rm e}^{2/3}$ at $0.1 \times R_{200}$ within each cluster. With the above definition, the quantity S relates to the thermodynamical entropy K of the system as $K \propto \log S$. In Figure 1.4, we plot the values of S as a function of the gas temperature. The predicted scaling of $S \sim T$ is in agreement with the overall fit of the data [$S = (427 \pm 20) \times T_{\rm gas}^{0.96 \pm 0.21}$ keV cm^2]. No significant evolution ($B = -0.05 \pm 0.05$, $\chi^2_{\rm min} = 101$ with 25 degrees of freedom) is observed when all our sample is compared with the *local* estimate of the "entropy ramp" by Ponman et al. (2003; see Fig. 1.4, panel on the left). However, the high χ^2 value warns that this is not a good modelization of the data distribution, mainly for their large internal scatter. If we consider only the objects at $z > 0.6, 0.8$ and 1, respectively, we observe consistently $B \approx 0.3$ with a deviation from no evolution at the $2-3\sigma$ confidence level, with a reduced χ^2 of about 1. In Ettori et al. (2003b),

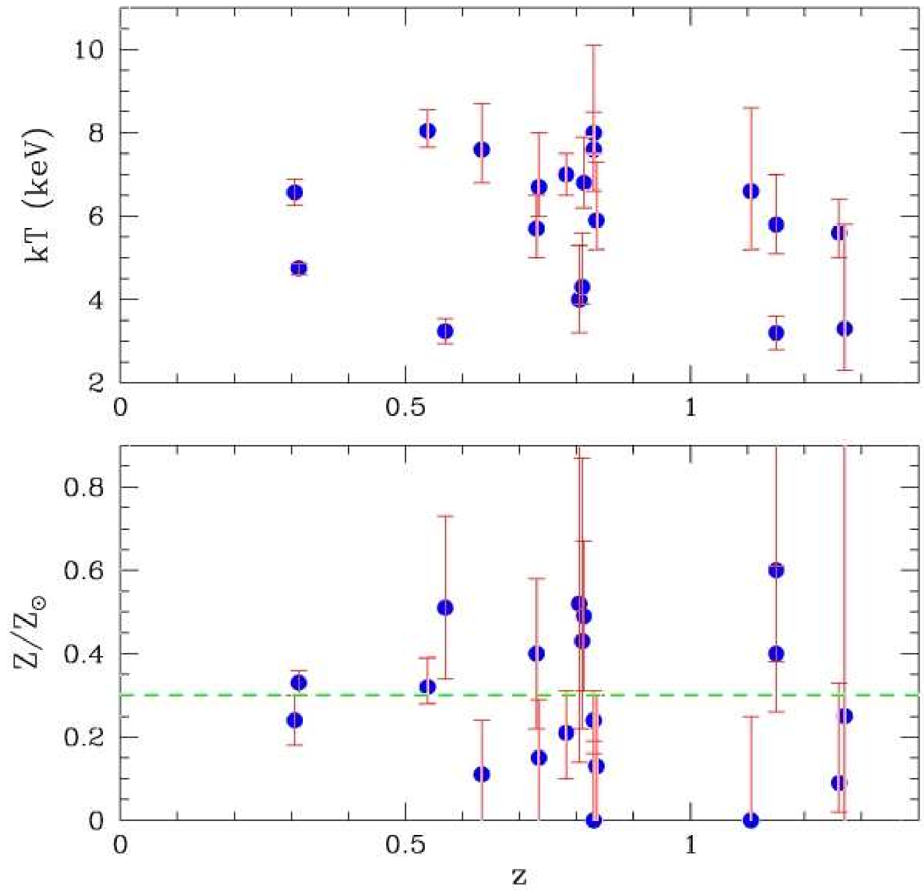

Fig. 1.3. Temperature *(upper panel)* and Iron abundance *(lower panel)* vs. redshift for the 18 clusters (2 of these double) in the sample. Error bars refer to 1σ. Spearman's rank coefficient indicates no-correlation both in the $(kT-z)$ plane and in the $(Z-z)$ plane. We detect, however, a trend significant at about 90% confidence level of lower Iron abundances in correspondence of higher temperatures ($kT > 5$ keV). The metallicity is given in units of the solar Fe abundances as measured in Anders & Grevesse (1989). At $z > 1$, we obtain a positive detection only for RXJ1053+5735 (observed only with *XMM-Newton*) and upper limits for the other three sources. We note that another positive detection ($Z = 0.36^{+0.12}_{-0.10} Z_\odot$) has been now observed in the *Chandra* -*XMM-Newton* long exposure of RXJ1252-2927, a 6.0 keV cluster at $z = 1.237$ as measured both optically and from the position of the detected Fe K line (Rosati et al. 2003).

we discuss how this positive evolution relates to the other scaling laws and how it might be explained as a combined effect of non–gravitational heating and radiative cooling.

References

Anders, E., & Grevesse, N. 1989, Geochimica et Cosmochimica Acta, 53, 197
Burles, S., Nollett, K.M., & Turner, M.S. 2001, ApJ, 552, L1
Ettori, S., De Grandi, S., & Molendi, S. 2002, A&A, 391, 841

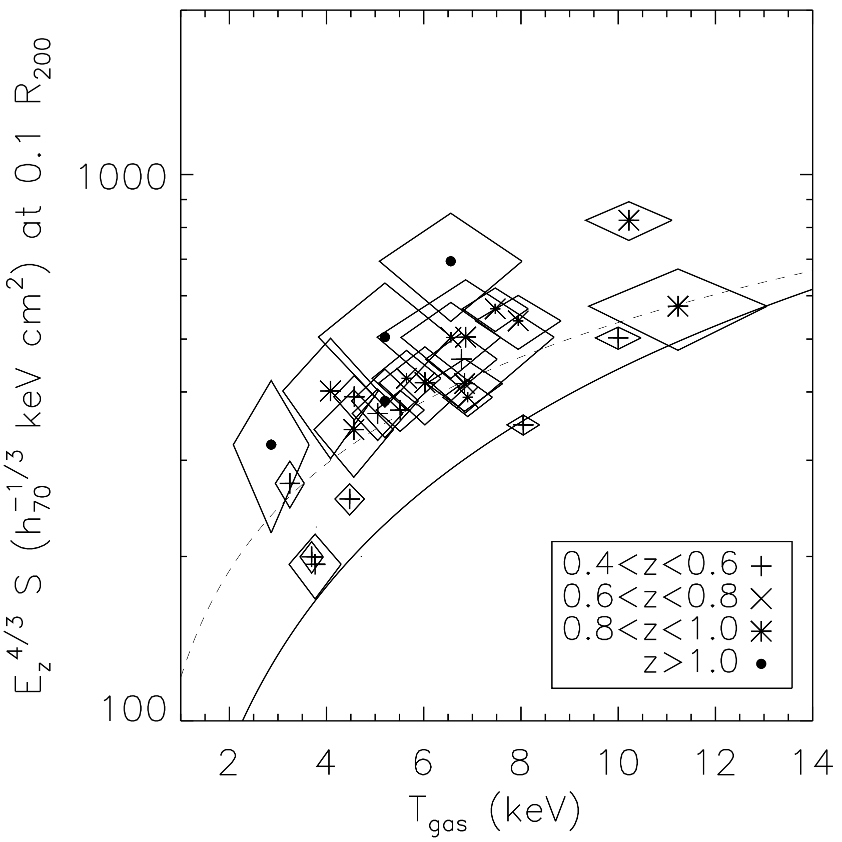

Fig. 1.4. Distribution of the entropy values measured at $0.1 \times R_{200}$ versus gas temperature. A rescaling factor of $E_z^{4/3}$ is used to compare these values to what is expected from hydrodynamical simulations, $S \approx 50\,(f_{\rm gas}/0.106)^{-2/3}\,T_{\rm keV}\,h_{70}^{-4/3}$ kev cm^2 (solid line, from Ponman et al. 1999 and normalized to the median gas fraction measured in our sample; dashed line, $S \approx 120\,T_{\rm keV}^{0.65}$, from Ponman et al. 2003).

Ettori, S., Tozzi, P., & Rosati, P. 2003a, A&A, 398, 879
Ettori, S., Tozzi, P., Borgani, S., & Rosati, P. 2003b, A&A, submitted
Freedman, W. et al. 2001, ApJ, 553, 47
Garnavich, P. et al. 1998, ApJ, 509, 74
Leibundgut, B., 2001, ARAA, 39, 67
Peebles, P.J.E., & Ratra, B., 2002, astro-ph/0207347
Ponman, T.J., Cannon, D.B., & Navarro, J.F. 1999, Nature, 397, 135
Ponman, T.J., Sanderson, A.J.R., & Finoguenov A. 2003, MNRAS, 343, 331
Press, W.H. 1996, in “Unsolved Problems in Astrophysics", Proceedings of Conference in Honor of John Bahcall, J.P. Ostriker ed., Princeton University Press (astro-ph/9604126)
Rosati, P. et al. 2003, AJ, in press
Sasaki, S. 1996, PASJ, 48, L119
Tozzi, P., Rosati, P., Ettori, S., Borgani, S., Mainieri, V., & Norman, C. 2003, ApJ, 593, 705

Wang, L., & Steinhardt, P.J. 1998, ApJ, 508, 483
White, S.D.M., Navarro, J.F., Evrard, A.E., & Frenk, C.S. 1993, Nature, 366, 429